Vision Research 178 (2021) 79–85

Contents lists available at ScienceDirect

Vision Research

journal homepage: www.elsevier.com/locate/visres

Blind spot and visual field anisotropy detection with flicker pupil perimetry across brightness and task variations

Brendan L. Portengen [a,b,1,*], Carlien Roelofzen [b,c,d,1], Giorgio L. Porro [a], Saskia M. Imhof [a], Alessio Fracasso [b,d,e], Marnix Naber [b]

[a] Ophthalmology Department, University Medical Center Utrecht, The Netherlands
[b] Experimental Psychology, Helmholtz Institute, Utrecht University, The Netherlands
[c] Experimental and Applied Psychology, VU University Amsterdam, The Netherlands
[d] Spinoza Centre for Neuroimaging, Amsterdam, The Netherlands
[e] Institute of Neuroscience and Psychology, University of Glasgow, Glasgow, United Kingdom

ARTICLE INFO

Keywords:
Perimetry
Pupillometry
Visual field
Blind spot

ABSTRACT

The pupil can be used as an objective measure for testing sensitivities across the visual field (pupil perimetry; PP). The recently developed gaze-contingent flicker PP (gcFPP) is a promising novel form of PP, with improved sensitivity due to retinotopically stable and repeated flickering stimulations, in a short time span. As a diagnostic tool gcFPP has not yet been benchmarked in healthy individuals. The main aims of the current study were to investigate whether gcFPP has the sensitivity to detect the blind spot, and upper versus lower visual field differences that were found before in previous studies. An additional aim was to test for the effects of attentional requirements and background luminance. A total of thirty individuals were tested with gcFPP across two separate experiments. The results showed that pupil oscillation amplitudes were smaller for stimuli presented inside as compared to outside the blind spot. Amplitudes also decreased as a function of eccentricity (i.e., distance to fixation) and were larger for upper as compared to lower visual fields. We measured the strongest and most sensitive pupil responses to stimuli presented on dark- and mid-gray backgrounds, and when observers covertly focused their attention to the flickering stimulus. GcFPP thus evokes pupil responses that are sensitive enough to detect local, and global differences in pupil sensitivity. The findings further encourage (1) the use of a gray background to prevent straylight without affecting gcFPPs sensitivity and (2) the use of an attention task to enhance pupil sensitivity.

1. Introduction

The diagnostic applicability of the dynamics of the eye's pupil has been a topic of research for various disciplines (Lussier, Olson, & Aiyagari, 2019; Naber, Alvarez, & Nakayama, 2013; Reuten, van Dam, & Naber, 2018; Wilhelm, Neitzel, Wilhelm, Beuel, Lüdtke, Kretschmann, & Zrenner, 2000). In experimental ophthalmological studies, the pupil is used for testing the visual field (VF) sensitivity using pupil perimetry (PP) (Carle, James, Kolic, Loh, & Maddess, 2011; Kardon, Kirkali, & Thompson, 1991; Schmid, Luedtke, Wilhelm, & Wilhelm, 2005). This application was developed to meet a demand for objective perimetry in ophthalmology, to examine patients who have difficulty cooperating with standard automated perimetry (SAP) (Wilhelm et al., 2000) and circumvent malingering. Our research group developed a novel form of PP, termed gaze-contingent flicker PP (gcFPP), which evokes multiple pupil responses by showing 2 Hz flickering stimuli across the VF. A gaze-contingent stimulus presentation ensures that the retinal location is fixed by use of an eye-tracker. A gaze-contingent stimulus presentation can correct for saccades online. We have demonstrated its potential in detecting large VF defects caused by cerebral visual impairment and glaucoma (Naber et al., 2018). Its high diagnostic sensitivity compared to other PP paradigms stems from more measurements in shorter time spans and accurate retinotopic stimulation with gaze-contingent stimulus presentations. Flicker perimetry has been applied before (Luu et al., 2013; Phipps, Dang, Vingrys, & Guymer, 2004). However, these studies chose a high flicker frequency (12–18 Hz) rather than a slow frequency

* Corresponding author at: Department of Ophthalmology, University Medical Center Utrecht, PO Box 85500, Room E 03.136, 3508 GA Utrecht, The Netherlands.
E-mail address: B.L.Portengen-2@umcutrecht.nl (B.L. Portengen).
[1] Shared first author.

https://doi.org/10.1016/j.visres.2020.10.005
Received 19 June 2020; Received in revised form 29 September 2020; Accepted 14 October 2020
Available online 5 November 2020
0042-6989/© 2020 The Authors. Published by Elsevier Ltd. This is an open access article under the CC BY license (http://creativecommons.org/licenses/by/4.0/).

(2 Hz) as in the current study. Using a low frequency evokes a sequence of pupil oscillations, while a high frequency evokes a single pupil constriction, a stimulus paradigm equivalent to static perimetry.

Our first aim is to test whether the gcFPP protocol is capable of detecting subtle differences in VF testing to further confirm its usefulness in testing VF sensitivities beyond patients with large scotomas. One way to ascertain gcFPP's sensitivity is by detecting the reduced pupil sensitivities in the blind spot (i.e., the punctum caecum; a retinal location without photoreceptor cells where the optic nerve passes through the optics disc towards the brain). Another manner to assess the sensitivity of gcFPP is to measure how well pupil oscillation amplitudes can be used to detect VF anisotropies, such as identifying higher sensitivities to light changes in upper as compared to bottom VFs (Hong, Narkiewicz, & Kardon, 2001; Naber et al., 2018; Sabeti, James, & Maddess, 2011; Skorkovská, Wilhelm, Lüdtke, Wilhelm, & Kurtenbach, 2014; Tan, Kondo, Sato, Kondo, & Miyake, 2001; Wilhelm et al., 2000). The detection performance of the blind spot and anisotropies can best be examined in healthy participants rather than patients for practical reasons. Healthy participants are easier to recruit and can withstand higher testing demands such as relatively long examinations. The subjective visibility ratings by the healthy observers will then serve as ground truth for comparison to pupil response amplitudes in and around the blind spot.

Our second aim is to test for the effects of design and contextual factors that may interfere or enhance its sensitivity. For example, PP stimuli are typically presented on a black background (Skorkovská, Lüdtke, Wilhelm, & Wilhelm, 2009) in order to maximize visual contrast and therewith pupil oscillation amplitudes. However, dark backgrounds tend to reduce the threshold for photo-sensitive retinal cells to respond, leading to unwanted activation due to stray light (e.g., a stimulus presented in the blind spot may still stimulate sensitive regions surrounding the blind spot due to light scatter). To circumvent this, our gcFPP protocol uses a (mid) gray background. However, it is currently unknown to what degree the increase of background luminance has detrimental effects on pupil sensitivity. A brighter background prevents straylight but also lowers Michelson contrast between the flickering stimulus and background and thus the pupil's responsiveness. We set to examine the ideal background illumination to minimize stray light effects and maximize pupil oscillation amplitudes in gcFPP.

Our third aim is to investigate the effects of the focus of attention of the observer. The pupillary light reflex does not only respond to retinal illumination. Instead, changes of pupil size are also modulated by top-down factors, such as the attentional state of the participant, with empirical evidence indicating that covert spatial attention can augment the pupillary responses (Binda & Murray, 2015; Binda, Pereverzeva, & Murray, 2013; Mathôt, van der Linden, Grainger, & Vitu, 2013; Naber et al., 2013; Naber & Nakayama, 2013). In our previous study (Naber et al., 2018), a covert attention detection task was used to evoke reliable pupil responses. A direct comparison between different attentional states in gcFPP has not yet been tested.

2. Methods

2.1. Participants

A total of thirty subjects participated in this study. One participant was excluded due to technical issues, resulting in twelve participants (11 females, age: $M = 22.3$, $SD = 2.3$) for Experiment 1 (blind spot detection), and eighteen tested observers (11 females, age: $M = 21.9$, $SD = 1.5$) for Experiment 2 (attention, luminance and visual field anisotropies). All participants were Dutch and reported having normal or corrected-to-normal visual acuity and having no visual disorders or neurological disorders. Participants were unaware of the purpose of the experiment and were only told that the eye-tracker measured their eye movements. Participants received financial reimbursement or study credit for participation, gave informed written consent on paper before the experiment, and were debriefed afterwards about the purpose of the experiment. This study conformed to the ethical principles of the Declaration of Helsinki, and was approved by the local ethical committee of the University Medical Center Utrecht (Approval number: 09/350).

2.2. Apparatus and stimuli

We used the same setup and stimuli for both experiments which were equivalent to those described by Naber et al. (2018). We generated stimuli on a Dell desktop computer with Windows 7 operating system (Microsoft, Redmond, Washington), MATLAB (Mathworks, Natick, MA, USA), and the Psychophysics toolbox extension (Brainard, 1997; Pelli, 1997). Stimuli were presented on an LED Asus ROG swift monitor (AsusTek Computer Inc., Taipei, Taiwan) that displayed 1920 by 1080 pixels at a 100 Hz refresh rate. The screen was 60 cm in width and 35 cm in height (320 cd/m^2 maximum luminance), and the participant's viewing distance to the screen was fixed at 55 cm with a chin and forehead rest. We recorded pupil size and gaze angle using an Eyelink 1000 eye-tracker camera (SR Research, Ontario, Canada; 0.5-degree accuracy of gaze location) that was placed 40 cm in front of the participant below the screen. For the eye-tracker calibration we used a thirteen-point calibration grid which took ~ 3 min per eye. Both experiments were conducted in a darkened room without ambient light.

2.2.1. Experiment 1 – blind spot detection

The stimuli (see Fig. 1**a and b**) consisted of (i) a black and white bull's eye that was used to ensure fixation (0.4 degree radius), (ii) a flickering disk that was presented on a dark gray background (80 cd/m^2) at separate locations per trial (randomized) centered around the estimated location of the blind spot (14 degrees from the vertical meridian; 2 degrees below the horizontal meridian; Wang et al., 2017), and (iii) a 2 Hz stream of characters superimposed on the disk for a letter detection task to ensure participants remained engaged with each stimulus (see Fig. 1; also see Naber et al., 2013 for details). When testing the left eye, the fixation point was placed on the right side (7.5 deg from the screen's center) of the screen and vice versa for the right eye. We used a gaze-contingent paradigm, meaning that the disk locations were corrected online with the same angle and amplitude read-out from the eye-tracker to ensure a stable flicker stimulation in retinal coordinates (also see Naber et al., 2018). Flicker rate was set at 2 Hz with a square wave step, and the change in stimulus luminance was between black at 0.01 cd/m^2 and white at 320 cd/m^2 luminance. The flickering disk had a width of 3.5 degrees in visual angle. The physiological blind spot typically has a width of 8- and height of 10 degrees in visual angle (Armaly, 1969; Safran, Mermillod, Mermoud, Weisse, & Desangles, 1993). Experiment 1 consisted of 130 trials (65 stimulus location; one block for pupil measurements, another block for visibility ratings). Trials were randomized and each trial consisted of one stimulus presentation for 6 s.

2.2.2. Experiment 2 – attention, luminance and visual field anisotropies

For experiment 2, we used the same stimuli but the locations of the stimuli were centered at a 9-degree maximum eccentricity around fixation that consisted of a black and white bull's eye (see Fig. 1**a and c**). Furthermore, the flickering disk that was presented on a light gray background (240 cd/m^2), mid gray background (160 cd/m^2) or dark gray background (80 cd/m^2). The stream of characters was either not shown, shown at fixation, or shown on top of the flickering disk (see Procedure for details) For this experiment, the flickering disk was increased to a width of 4 degrees in visual angle to increase pupil sensitivity. Experiment 2 consisted of 432 trials (3 attention conditions × 3 luminance conditions × 48 stimulus locations). Trials were randomized and each trial consisted of one stimulus presentation for 2 s.

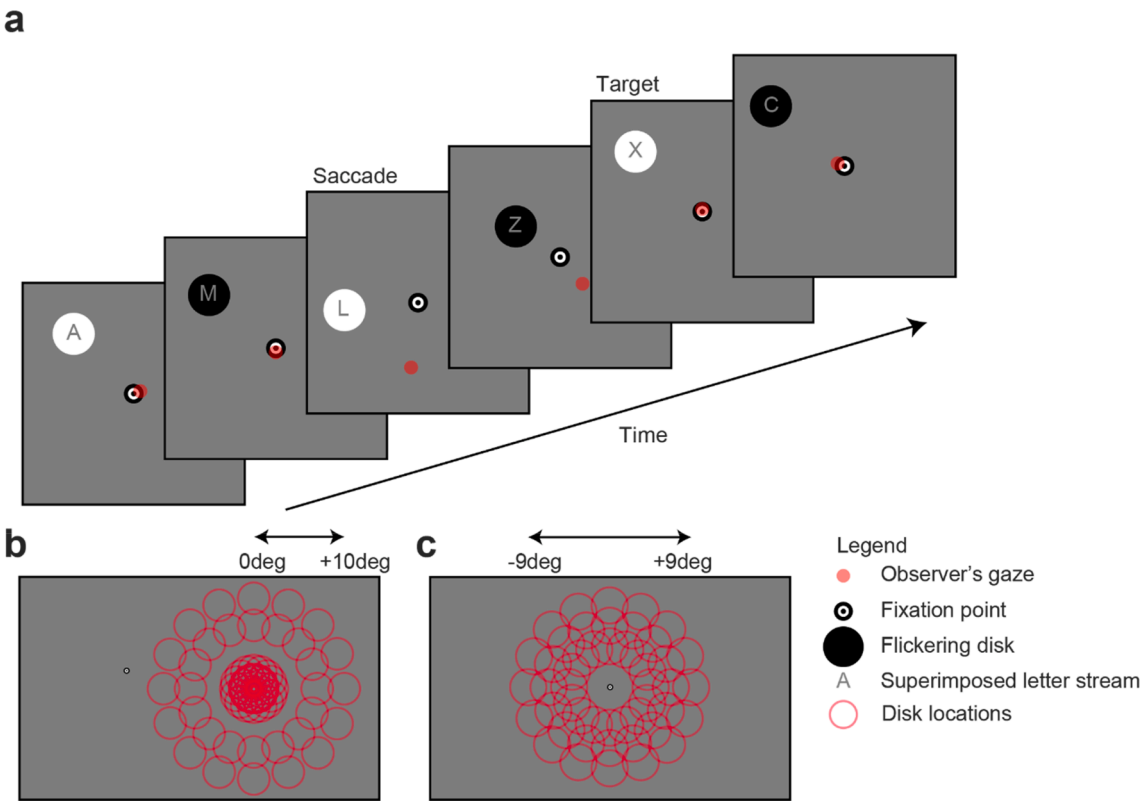

Fig. 1. Procedure and stimuli. (a) Procedure: observers fixated the bull's eye, while the flickering disk was presented in the periphery. A gaze-contingent stimulus presentation was used to ensure that the retinal location of the stimulus was fixed. (b) Stimulus locations experiment 1: the flickering disk was located at 5 radial distances from the blind spot's center (0-, 1-, 2-, 7-, and 10-degree eccentricity, 16 angles). The bull's eye was placed on the left side of the screen when testing the right eye and vice versa. (c) Stimulus locations experiment 2: the flickering disk was located at 3 radial distances (4.5-, 6.75-, and 9-degree eccentricity, 16 angles).

2.3. Procedure

Participants were tested on varying times of the day. Eye dominance was tested by using the "hole-in-the card test" (Ding, Naber, Gayet, van der Stigchel, & Paffen, 2018). Five out of eleven in exp. 1 and four out of seventeen in exp 2 had left eye dominance. Depending on left and right eye dominance, stimuli were either presented in and around the blind spot that was located right or left from fixation in experiment 1, respectively. Due to the lacking information on how the Eyelink software calculates pupil size, we could only roughly estimate participants' average pupil sizes (M = 4.9 mm, SD = 1.1 mm) and standard deviation across trial time (M = 0.03 mm, SD = 0.01 mm) in millimeters (As a reference pupil, we held a black dot with a fixed radius drawn on a piece of paper in front of the camera at the same distance as the eyes of our participants).

2.3.1. Experiment 1 – blind spot detection

The non-dominant eye of the participant (counterbalanced) was patched with a black eye patch to ensure monocular viewing with the dominant eye. In the subjective part of the experiment we asked the participants to rate the visibility of each flickering disk on a 11-point Likert scale (0 = fully invisible, 10 = fully visible), whereas in the objective part of the experiment we asked the participants to fixate the bull's eye. No letters were shown during the subjective part of experiment 1 to prevent participants from reporting letter visibility instead of disk visibility.

2.3.2. Experiment 2 – attention, luminance and visual field anisotropies

Participants viewed the stimuli binocularly. To better understand how instructions and task requirements affect the accuracy of gcFPP, we also investigated the effect of attention on the sensitivity of pupil responses. Three attention tasks were tested in different blocks. In the passive attention task, participants only fixated the bull's eye. For the distracted attention task, participants were instructed to silently count the number of appearances of a letter 'X' among the stream of letters, changing at a rate of 2 Hz, presented at the center of the bull's eye. Participants indicated how many X's they had seen after all trials. For the covert attention task, those letters were instead superimposed on the stimulus disk and participants had to covertly attend the X's while maintaining fixation at the bull's eye.

2.4. Analysis

First, we detected and removed blink episodes from the pupil data by setting a speed threshold of >4SD above the mean. Blink episodes were interpolated with a cubic method. Each recorded pupil trace was transformed per observer from pupil size as a function of time during the experiment to 3000 ms epochs of pupil size measurements with respect to each stimulus onset. The resulting multiple pupil size traces were then band-pass filtered to remove low- (subtraction of a 2nd order fit with 1 Hz cut-off frequency) and high-frequency (replacing with a 5th order fit with 15 Hz cut-off frequency) noise, baseline corrected (through lowpass fit subtraction) and z-normalized to enable comparisons across participants, checked for trial outliers (>3 SD above the mean) in variance across locations (average of 1.4% ± 0.7% of stimulus trials excluded per observer), and assigned to a condition matrix. Note that the Eyelink tracker software outputs pupil size in arbitrary units rather than absolute pupil diameter in millimeters.

The resulting pupil data matrices per condition were transformed to the frequency spectrum domain with a fast Fourier transform (FFT) per 3000 ms stimulus trial. The resulting spectrum contained power values around the target frequency of 2 Hz for 21 different frequencies between

0 and 4 Hz. The pupil oscillation power at 2 Hz, computed by taking the maximum power within a range of 1.6–2.4 Hz to capture small deviations from the target frequency, served as the reference measurement of pupil response amplitude to each 2 Hz flickering stimulus per VF location. This measure was shown to have highest sensitivity in detecting differences in pupil sensitivity (Naber et al., 2018).

Two-dimensional high-resolution pupil sensitivity maps (e.g., see Fig. 2**c**) were created with MatLab's biharmonic spline interpolation across visual field locations. Comparisons in pupil sensitivities between inside versus outside the physiological blind spot were made by calculating the area under the curve (AUC; range: 0.5–1.0; for more info, see (Macmillan & Creelman, 2004)) on pupil oscillation amplitudes. An AUC of 0.5 means that the amplitude value distributions of the blind spot and the rest of the tested visual field fully overlap (i.e., not dissociable; no sensitivity) while an AUC of 1.0 means that the compared distributions are fully dissociable (i.e., a high sensitivity). Paired double-sided t-tests were conducted to statistically assess whether amplitudes and AUC's differed significantly across VF locations. Reported correlations are of type Pearson's rho. To determine statistical significance of differences in amplitudes and AUC's across eccentricities, attention tasks, and background brightness's, repeated measures ANOVA and paired double-sided t-tests were conducted. Fig. 2a and c were calculated with the following analysis steps: First, we created a sensitivity map per participant. Second, we horizontally flipped the heatmaps of participants whoms left eye was tested (because of left eye dominance). Third, we averaged all maps across participants to a single average heat map. Fourth, the map was normalized such that black represents the minimum (Subjective visibility score: 0.4; pupil power exp 1: 0.1; exp 2: 2.0) and white the maximum (Subjective visibility score: 9.8; pupil power exp 1: 6.5; exp 2: 4.8).

3. Results

3.1. Results and discussion experiment 1 – blind spot detection

In experiment 1 we set to test whether we could locate the physiological blind spot by means of detecting a decrease in pupil power. First, we located the blind spot by examining the subjective visibility ratings by observers across the VF (Fig. 2**a**). A significant decrease in visibility ratings was observed for the expected locations inside the blind spot as compared to outside the blind spot (Fig. 2**b**; $t(11) = 13.32$, $p < 0.001$). On average the actual blind spot location was slightly shifted to the right as compared to our expectations and thus from the probed locations, meaning that we underestimated the eccentricity of the blind spot. Note, however, that the blind spot locations are more in line with studies mapping it 16 degrees rather than 14 degrees from the vertical axis (Armaly, 1969; Safran et al., 1993). The objective pupil powers plotted across the VF showed a similar pattern as the subjective visibility ratings (Fig. 2**c**). Pupil powers also correlated significantly with visibility ratings ($M = 0.28$, $SD = 0.19$; $t(11) = 4.59$, $p < 0.001$). To test for differences in pupil powers between inside and outside blind spot regions, we divided the VF based on the visibility ratings by using a 50% percentile threshold per observer. Pupil power was significantly lower for stimuli presented inside as compared to outside the rating-based blind spot regions (Fig. 2**d**; $t(11) = 4.06$, $p = 0.001$) and the area under the curve also scored significantly above chance (Fig. 2**e**; $t(11) = 8.75$, $p < 0.001$). To summarize the results, we found that gcFPP has a sensitivity that is sufficient to detect the blind spots in healthy observers, suggesting that it can potentially be used to detect relatively small scotomas in patients with VF defects.

3.2. Results and discussion experiment 2 – attention, luminance and visual field anisotropies

We first inspected whether the 2 Hz flickering stimuli evoked the expected oscillatory pattern in the pupil traces. As shown in Fig. 3**a** this expectation was confirmed. Pupil size oscillated at a rate of approximately 2 Hz. Next we investigated whether the amplitudes of these oscillations, measured as the signal power at 2 Hz frequency in the Fourier domain, varied across the background brightness and attention task conditions. The pupil power varied substantially across conditions (Fig. 3**b**), with the largest observed for a dark gray background with attention directed to the flickering disk. A two-way repeated measures ANOVA indicated that pupil power significantly varied as a function of background brightness (BB) attention task (AT), no interaction was observed (BB: $F(2,32) = 31.09$, $p < 0.001$; AT: $F(2,32) = 5.46$, $p = 0.009$; BB*AT: $F(4,64) = 1.99$, $p = 0.106$. Next, we examined whether the above-mentioned conditions performed best at detecting VF anisotropies. Typical VF anisotropies in pupil perimetry consist of a decrease in pupil responsiveness for peripheral as compared to foveal and superior (i.e., upper) as compared to inferior (i.e., lower) VFs (Hong et al., 2001; Naber et al., 2018; Skorkovská et al., 2014; Tan et al., 2001)[2]. We first plotted pupil power across stimulus locations as a heat map (Fig. 3**c**). As further confirmed in repeated measures ANOVAs, pupil power varied significantly across eccentricities (Fig. 3**d**; $F(2,32) = 46.76$, $p < 0.001$) and post-hoc comparisons indicated a decrease in pupil amplitudes as eccentricity (i.e., distance to fixation) increases (Table S1). Pupil amplitudes were also significantly stronger in upper as compared to low VFs (Fig. 3**e**; $F(2,16) = 16.41$, $p < 0.001$; for post-hoc statistics, see Table S2). Using signal detection theory, we calculated the sensitivity of pupil power as a measure to dissociate between lower and upper VFs (Fig. 3**f**), which is a comparison most representative to VF defects of patients in clinical practice. Anisotropy detection sensitivity, operationalized as the area under the curve of a receiver-operator characteristic (AUC; see Methods – Analysis for details) varied significantly across background brightness conditions with largest sensitivity for the dark gray and mid gray backgrounds ($F(2,16) = 3.56$, $p = 0.040$; for post-hoc comparisons, see Table S3). Sensitivities did not vary significantly across attention tasks ($F(2,16) = 2.24$, $p = 0.123$). To conclude, gcFPP achieved highest sensitivity as a measure to detect VF anisotropies when stimuli were presented on a relatively dark gray background.

4. General discussion

The main objectives of this study were (i) to estimate how successful gcFPP is in detecting the blind spot and VF anisotropies in healthy individuals and (ii) to examine maximum pupil sensitivity across background illuminations and (iii) task designs.

To our knowledge this is the first study that benchmarked PP's capability to detect the blind spot. Previous research, however, already used the physiological blind spot as a proxy of a small scotoma to assess other non-pupillometric perimetry techniques (Asman et al., 1999; Bek & Lund-Andersen, 1989; Mutlukan & Damato, 1993). Measuring the blind spot in healthy participants allowed us to test participants for longer time periods than possible with patients that have pathological scotomas. Our current and previous findings (Naber et al., 2018) show gcFPP can detect small scotomas like the physiological blind spot and larger defects such as hemianopia in patients suffering from cerebral visual impairment or glaucoma, suggesting gcFPP could be a viable objective alternative to SAP. It should, however, be noted that there was a decrease in sensitivity below the blind spot in Fig. 2c. This could possibly result from variabilities in photoreceptor cell densities, the cortical magnification factor, or variations in luminance across the LCD screen.

Regarding VF anisotropies, previous studies found strongest pupil responses in the center of the VF, weaker responses in the periphery, and

[2] We could not assess the visual field anisotropy of temporal (i.e., towards the temples) versus nasal (i.e., towards the nose) locations because in Experiment 2 observers watched the stimuli binocularly.

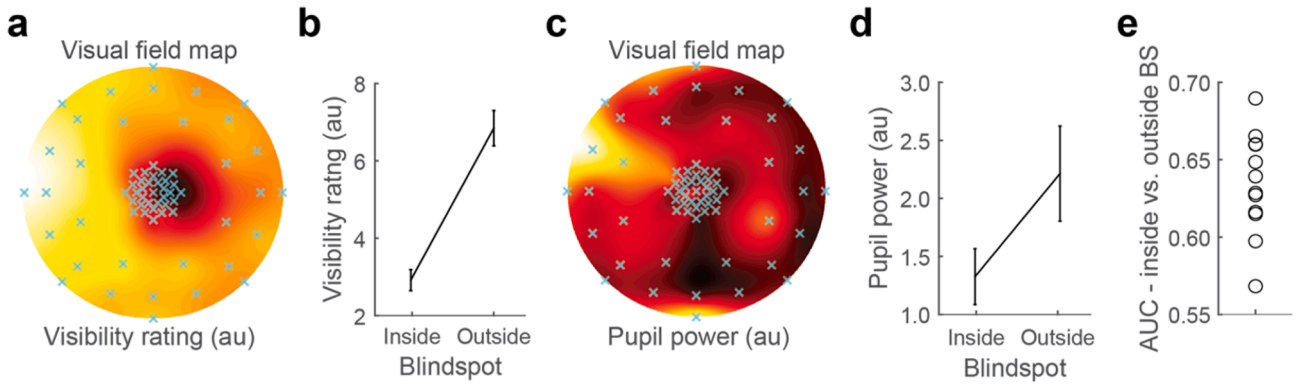

Fig. 2. Results. (a) Heatmap of visibility ratings around blind spot averaged across observers. Brighter (or hotter) colors indicate stronger pupil oscillation amplitudes. Note that the colors represent arbitrary values. Black and white values reflect the normalized lower (black) and upper (bright) limits of visibility ratings per observer, respectively. Also note that fixation was either on the left or right, outside the plot and is not displayed here. (b) Visibility ratings for inside versus outside blind spot location averaged across observers. Error bars indicate the standard error of the mean. (c) Heatmap of pupil powers around blind spot averaged across observers. (d) Pupil power for inside versus outside blind spot locations. (e) Area under the curve (AUC) of signal detection's receiver operator characteristic that compared pupil power distributions of inside versus outside blind spot locations (BS) across observers.

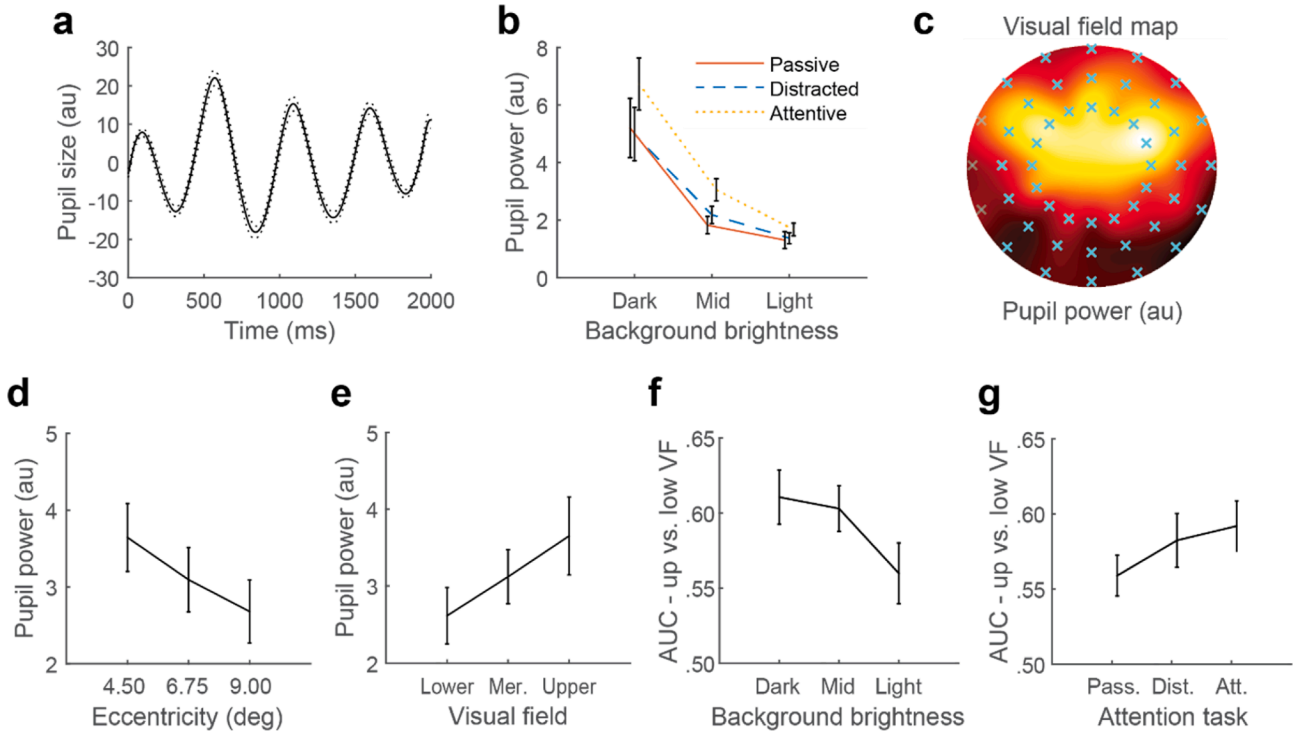

Fig. 3. Results. (a) Pupil oscillations averaged across observers. The dotted lines indicate the standard error from the mean. (b) Pupil oscillation power per background brightness (x-axis) and covert attention condition (colors; legend). (c) Heatmap of relative pupil power across the visual field (VF) averaged across all conditions and averaged across observers. Brighter (or hotter) colors indicate stronger pupil oscillation amplitudes. The minimum (black) and maximum (white) pupil amplitudes varied across observers. This plot represents the average of amplitudes, which values were normalized to a fixed range per observer. Note that observers fixated the center of the plot and the cyan crosses indicate the locations of the stimuli. (d) Pupil power per stimulus eccentricity in visual degrees. (e) Pupil power lower to upper visual regions. (f) Area under the curve (AUC) of signal detection's receiver operator characteristic that compared pupil power distributions of upper and lower VFs averaged across observers per background luminance (black) and (g) attention condition (gray). (For interpretation of the references to colour in this figure legend, the reader is referred to the web version of this article.)

stronger pupil responses in the upper and temporal than lower and nasal VFs, respectively (Hong et al., 2001; Naber et al., 2013, 2018; Sabeti et al., 2011; Skorkovská et al., 2014; Tan et al., 2001; Wilhelm et al., 2000). Our results are consistent with these previous observations.

We have also found that flickering stimuli presented over a dark-gray background evoked the strongest pupil responses as opposed to mid- and light-gray backgrounds. Furthermore, attended rather than unattended stimuli evoked strongest pupil responses to flickering on- and offsets. Surprisingly, different attentional conditions and background levels had comparable sensitivities in detecting VF anisotropies. This suggests that the selection of background luminance below 160 cd/m^2 and the type of attention task does not greatly impact gcFPP sensitivity.

PP has the potential to meet the demand for an objective alternative to SAP, which is the current golden standard for testing the VF. However, multiple variants of PP currently exist; the gcFPP (Naber et al., 2018) of the current study, unifocal PP (e.g., Schmid et al., 2005), in

which a single stimulus appears at a given retinotopic location once, and multifocal PP (e.g., Wilhelm et al., 2000), which stimulates multiple retinotopic locations simultaneously. Future studies are needed to compare the sensitivities across methods using a common paradigm. Additionally, test–retest variability needs to be tested to examine PP's diagnostic accuracy.

This study focused on optimizing pupil responses to visual stimuli by ways of changing background luminance and manipulating the degree of attention for these stimuli. Other interesting stimulus design factors that could be considered to improve gcFPP are spatial and temporal sparseness; i.e. optimizing the pupillary response by changing the number of stimuli shown simultaneously across the VF (spatial sparseness) and the frequency of presentations within a certain time window (temporal sparseness). The current gcFPP protocol only shows a single stimulus repeatedly (high spatial sparseness, low temporal sparseness), while Sabeti et al. (2011) showed that high spatial and temporal sparseness resulted in better performance with multifocal PP. One of the characteristics of the 2 Hz flicker used in this study is its low temporal sparseness (i.e., relatively many stimulus changes). This frequency was chosen to increase the amount of pupillary measurements within a relatively short time window (Naber et al., 2018), but a higher temporal sparseness (i.e., lower frequency) could possibly result in stronger pupil responses. More investigations into these stimulus factors will be needed to find the optimum diagnostic sensitivity.

Our results show that when observers conduct a detection task with letters superimposed on the flickering target stimulus, larger pupil responses are evoked than when observers perform a distraction task at fixation or passively view a fixation dot. This is in line with literature showing that increased focused attention on the target stimulus results in enhanced pupillary responses (Binda & Murray, 2015; Binda et al., 2013; Binda, Pereverzeva, & Murray, 2014; Carrasco, Ling, & Read, 2004; Laeng & Endestad, 2012; Mathôt et al., 2013; Naber et al., 2013; Naber & Nakayama, 2013). Based on these results it is tempting to suggest that drawing covert attention to the stimuli improves gcFPP's diagnostic sensitivity. However, the results also showed that the sensitivity in detecting upper vs lower visual field anisotropies does not differ along several attentional conditions. The question remains whether this inconsistency generalizes to the detection of – much less subtle – scotomas. Nonetheless, adding an additional task in the same position of the stimulus is not detrimental for gcFPP's sensitivity and makes the task more engaging for observers.

Note that the perimetry method was benchmarked based on its sensitivity in dissociating pupil amplitude values of upper versus lower VFs in healthy individuals. Stimuli were however always visible to the observer, a situation which is not comparable to clinical practice. GcFPP can also be used to map the regions in the VFs where stimuli are not detected by the observer in patients with an absolute scotoma (Naber et al., 2018).

This study had some limitations. The first one concerns our gcFPP protocol, because only stimuli with the same size at all eccentricities were used. For clinical and/or diagnostic purposes the stimuli should be corrected for the cortical magnification factor and the density distributions of the photoreceptor cell types to take into account eccentricity effects and therewith to more accurately assess the VF in patients.

Another limitation concerned the background. This study investigated the optimal background luminance for gcFPP. Three backgrounds were tested; a light-, mid-, and dark gray background. Although the objective of the study was to assess differences across different shades of gray, which all prevent stray light to some degree, a black background condition could have served as a useful control condition. However, there are three reasons we did not add it to the current study. First, an extra condition would prolong test duration. Second, we were mainly interested in exploring lighter backgrounds and whether these would lead to more specific results. Third, and most importantly, LCD screens have a very long persistence with a white-on-black stimulus (Lagroix, Yanko, & Spalek, 2012).

In our current and previous pupil perimetry protocols, stimulus size was always around 4 visual degrees. It is important to note that standard perimetry uses much smaller ~0.5 degree stimulus sizes, allowing VF testing at a much higher spatial resolution. An increase in stimulus size at the expense of spatial resolution must be made to ensure strong enough responses in pupil perimetry. Consequently, PP is probably not accurate at detecting small scotomas (<3 degrees). Additionally, PP cannot detect full field deficits present in both eyes because then within field comparisons will not show large differences in pupil sensitivity.

Although the objective pupil powers plotted across the VF did not show an identical pattern, analysis showed that it was possible to predict the blind spot. The darker regions outside the blind spot can be attested to the VF anisotropies generally found in pupil perimetry. Furthermore, Fig. 2b and d show standard error bars; standard deviations, which measures variability from the individual data values to the mean, would raise applicability for clinical use.

As described in a paper by Ghodrati and colleagues (Ghodrati, Morris, & Price, 2015), LCD screens are not really homogenous in luminance across the screen. Note, however, that the stimuli surrounding the blind spot were closer to the center of the screen than the edge and potentially changes position erratically due to the gaze contingent nature of the design. Following from this, the results can hardly be explained by potential inhomogeneities of the LCD.

Last, the current results could be biased by the overrepresentation of women and young adults in our sample. While no gender differences in pupil responses to these types of stimuli have so far been reported in the literature, age norms should be developed prior to clinical use of PP.

To conclude, we have demonstrated gcFPP's usefulness in detecting local and global differences in pupil sensitivity and we recommend to use dark to mid gray backgrounds and to ensure observer's attention to stimuli with task-relevant targets.

CRediT authorship contribution statement

Brendan L. Portengen: Writing - original draft, Writing - review & editing. **Carlien Roelofzen:** Investigation, Writing - original draft. **Giorgio L. Porro:** Supervision, Writing - review & editing. **Saskia M. Imhof:** Supervision. **Alessio Fracasso:** Project administration, Writing - review & editing. **Marnix Naber:** Conceptualization, Software, Supervision, Formal analysis, Writing - original draft, Writing - review & editing.

Declaration of Competing Interest

The authors declare that they have no known competing financial interests or personal relationships that could have appeared to influence the work reported in this paper.

Acknowledgments

Funding: This work was supported by a grant from UitZicht (grant 2017-18, fund involved: the Rotterdamse Stichting Blindenbelangen [grant number B20170004]), and grants from the ODAS foundation [grant number 2017-03]; and the F.P. Fischer Foundation [grant number 170511]), and a grant from the Janivo Foundation [grant number 2017170]. A.F. is supported by a grant from the Biotechnology and Biology research council (BBSRC, grant number: BB/S006605/1) and a grant from UitZicht (grant 2016-35, funds involved: F.P. Fischer Foundation, Stichting Glaucoomfonds, LSBS fund and Oogfonds). M.N. is supported by a grant from UitZicht (grant 2018-10, fund involved: Rotterdamse Stichting Blindenbelangen).

Appendix A. Supplementary data

Supplementary data to this article can be found online at https://doi.org/10.1016/j.visres.2020.10.005.

References

Armaly, M. F. (1969). The size and location of the normal blind spot. *Archives of Ophthalmology, 81*(2), 192–201. https://doi.org/10.1001/archopht.1969.00990010194009.

Asman, P., Fingeret, M., Robin, A., Wild, J., Pacey, I., Greenfield, D., … Ritch, R. (1999). Kinetic and static fixation methods in automated threshold perimetry. *Journal of Glaucoma, 8*(5), 290–296. http://www.ncbi.nlm.nih.gov/pubmed/10529927.

Bek, T., & Lund-Andersen, H. (1989). The influence of stimulus size on perimetric detection of small scotomata. *Graefe's Archive for Clinical and Experimental Ophthalmology, 227*(6), 531–534. https://doi.org/10.1007/BF02169446.

Binda, P., & Murray, S. O. (2015). Spatial attention increases the pupillary response to light changes. Journal of Vision, 15(2), 1–1. https://doi.org/10.1167/15.2.1.

Binda, P., Pereverzeva, M., & Murray, S. O. (2013). Attention to bright surfaces enhances the pupillary light reflex. *Journal of Neuroscience, 33*(5), 2199–2204. https://doi.org/10.1523/JNEUROSCI.3440-12.2013.

Binda, P., Pereverzeva, M., & Murray, S. O. (2014). Pupil size reflects the focus of feature-based attention. *Journal of Neurophysiology, 112*(12), 3046–3052. https://doi.org/10.1152/jn.00502.2014.

Brainard, D. H. (1997). The Psychophysics Toolbox. *Spatial Vision, 10*(4), 433–436. https://doi.org/10.1163/156856897X00357.

Carle, C. F., James, A. C., Kolic, M., Loh, Y.-W.-W., & Maddess, T. (2011). High-Resolution Multifocal Pupillographic Objective Perimetry in Glaucoma. *Investigative Ophthalmology & Visual Science, 52*(1), 604–610. https://doi.org/10.1167/iovs.10-5737.

Carrasco, M., Ling, S., & Read, S. (2004). Attention alters appearance. *Nature Neuroscience, 7*(3), 308–313. https://doi.org/10.1038/nn1194.

Ding, Y., Naber, M., Gayet, S., van der Stigchel, S., & Paffen, C. (2018). Assessing the generalizability of eye dominance across binocular rivalry, onset rivalry, and continuous flash suppression. *Journal of Vision, 18*(6). https://doi.org/10.1167/18.6.6.

Ghodrati, M., Morris, A., & Price, N. (2015). The (un)suitability of modern liquid crystal displays (LCDs) for vision research. *Frontiers in Psychology, 6*(MAR). https://doi.org/10.3389/fpsyg.2015.00303.

Hong, S., Narkiewicz, J., & Kardon, R. H. (2001). Comparison of Pupil Perimetry and Visual Perimetry in Normal Eyes: Decibel Sensitivity and Variability. *Investigative Ophthalmology & Visual Science, 42*(5), 957–965.

Kardon, R. H., Kirkali, P. A., & Thompson, H. S. (1991). Automated pupil perimetry pupil field mapping in patients and normal subjects. *Ophthalmology, 98*(4), 485–496. https://doi.org/10.1016/S0161-6420(91)32267-X.

Laeng, B., & Endestad, T. (2012). Bright illusions reduce the eye's pupil. Proceedings of the National Academy of Sciences of the United States of America, 109(6), 2162–2167. https://doi.org/10.1073/pnas.1118298109.

Lagroix, H. E. P., Yanko, M. R., & Spalek, T. M. (2012). LCDs are better: Psychophysical and photometric estimates of the temporal characteristics of CRT and LCD monitors. *Attention, Perception, and Psychophysics, 74*(5), 1033–1041. https://doi.org/10.3758/s13414-012-0281-4.

Lussier, B. L., Olson, D. W. M., & Aiyagari, V. (2019, October 1). Automated Pupillometry in Neurocritical Care: Research and Practice. Current Neurology and Neuroscience Reports. Current Medicine Group LLC 1. https://doi.org/10.1007/s11910-019-0994-z.

Luu, C. D., Dimitrov, P. N., Wu, Z., Ayton, L. N., Makeyeva, G., Aung, K. Z., … Guymer, R. H. (2013). Static and flicker perimetry in age-related macular degeneration. *Investigative Ophthalmology & Visual Science, 54*(5), 3560–3568. https://doi.org/10.1167/iovs.12-10465.

Macmillan, N. A., & Creelman, C. D. (2004). Detection Theory: A User's Guide: 2nd edition. Detection Theory: A User's Guide: 2nd edition. Psychology Press. https://doi.org/10.4324/9781410611147.

Mathôt, S., van der Linden, L., Grainger, J., & Vitu, F. (2013). The pupillary light response reveals the focus of covert visual attention. *PLoS ONE, 8*(10). https://doi.org/10.1371/journal.pone.0078168.

Mutlukan, E., & Damato, B. E. (1993). Computerised perimetry with moving and steady fixation in children. *Eye (Basingstoke), 7*(4), 554–561. https://doi.org/10.1038/eye.1993.121.

Naber, M., Alvarez, G. A., & Nakayama, K. (2013). Tracking the allocation of attention using human pupillary oscillations. *Frontiers in Psychology, 4*, 919. https://doi.org/10.3389/fpsyg.2013.00919.

Naber, M., & Nakayama, K. (2013). Pupil responses to high-level image content. Journal of Vision, 13(6), 7–7. https://doi.org/10.1167/13.6.7.

Naber, M., Roelofzen, C., Fracasso, A., Bergsma, D. P., van Genderen, M., Porro, G. L., … van der Schouw, Y. T. (2018). Gaze-contingent flicker pupil perimetry detects scotomas in patients with cerebral visual impairments or glaucoma. *Frontiers in Neurology, 9*(July), 558. https://doi.org/10.3389/fneur.2018.00558.

Pelli, D. G. (1997). The VideoToolbox software for visual psychophysics: Transforming numbers into movies. *Spatial Vision, 10*(4), 437–442. https://doi.org/10.1163/156856897X00366.

Phipps, J. A., Dang, T. M., Vingrys, A. J., & Guymer, R. H. (2004). Flicker perimetry losses in age-related macular degeneration. *Investigative Ophthalmology and Visual Science, 45*(9), 3355–3360. https://doi.org/10.1167/iovs.04-0253.

Reuten, A., van Dam, M., & Naber, M. (2018). Pupillary responses to robotic and human emotions: The uncanny valley and media equation confirmed. *Frontiers in Psychology, 9*(MAY). https://doi.org/10.3389/fpsyg.2018.00774.

Sabeti, F., James, A. C., & Maddess, T. (2011). Spatial and temporal stimulus variants for multifocal pupillography of the central visual field. *Vision Research, 51*(2), 303–310. https://doi.org/10.1016/J.VISRES.2010.10.015.

Safran, A. B., Mermillod, B., Mermoud, C., Weisse, C. D., & Desangles, D. (1993). Characteristic features of blind spot size and location, when evaluated with automated perimetry: Values obtained in normal subjects. *Neuro-Ophthalmology, 13*(6), 309–315. https://doi.org/10.3109/01658109309044579.

Schmid, R., Luedtke, H., Wilhelm, B. J., & Wilhelm, H. (2005). Pupil campimetry in patients with visual field loss. *European Journal of Neurology, 12*(8), 602–608. https://doi.org/10.1111/j.1468-1331.2005.01048.x.

Skorkovská, K., Lüdtke, H., Wilhelm, H., & Wilhelm, B. (2009). Pupil campimetry in patients with retinitis pigmentosa and functional visual field loss. *Graefe's Archive for Clinical and Experimental Ophthalmology, 247*(6), 847–853. https://doi.org/10.1007/s00417-008-1015-0.

Skorkovská, K., Wilhelm, H., Lüdtke, H., Wilhelm, B., & Kurtenbach, A. (2014). Investigation of summation mechanisms in the pupillomotor system. *Graefe's Archive for Clinical and Experimental Ophthalmology, 252*(7), 1155–1160. https://doi.org/10.1007/s00417-014-2677-4.

Tan, L., Kondo, M., Sato, M., Kondo, N., & Miyake, Y. (2001). Multifocal pupillary light response fields in normal subjects and patients with visual field defects. *Vision Research, 41*(8), 1073–1084. https://doi.org/10.1016/S0042-6989(01)00030-X.

Wang, M., Shen, L. Q., Boland, M. V., Wellik, S. R., De Moraes, C. G., Myers, J. S., … Elze, T. (2017). Impact of Natural Blind Spot Location on Perimetry. *Scientific Reports, 7*(1). https://doi.org/10.1038/s41598-017-06580-7.

Wilhelm, H., Neitzel, J., Wilhelm, B., Beuel, S., Lüdtke, H., Kretschmann, U., & Zrenner, E. (2000). Pupil Perimetry using M-Sequence Stimulation Technique. Investigative Ophthalmology & Visual Science, 41(5), 1229–1238.